

Kernel-based Joint Independence Tests for Multivariate Stationary and Nonstationary Time-Series

Zhaolu Liu¹, Robert L. Peach^{2,3} Felix Laumann¹,
Sara Vallejo Mengod¹ and Mauricio Barahona^{1*}

¹Department of Mathematics, Imperial College London, London, United Kingdom

²Department of Neurology, University Hospital Würzburg, Würzburg, 97070, Germany

³Department of Brain Sciences, Imperial College London, London, W12 0NN, United Kingdom,

*To whom correspondence should be addressed; E-mail: m.barahona@imperial.ac.uk

Abstract

Multivariate time-series data that capture the temporal evolution of interconnected systems are ubiquitous in diverse areas. Understanding the complex relationships and potential dependencies among co-observed variables is crucial for the accurate statistical modelling and analysis of such systems. Here, we introduce kernel-based statistical tests of joint independence in multivariate time-series by extending the d -variable Hilbert-Schmidt independence criterion (dHSIC) to encompass both stationary and nonstationary random processes, thus allowing broader real-world applications. By leveraging resampling techniques tailored for both single- and multiple-realization time series, we show how the method robustly uncovers significant higher-order dependencies in synthetic examples, including frequency mixing data, as well as real-world climate and socioeconomic data. Our method adds to the mathematical toolbox for the analysis of complex high-dimensional time-series datasets.

1 Introduction

Time series that record temporal changes in sets of system variables are ubiquitous across many scientific disciplines¹, from physics and engineering² to biomedicine^{3,4}, climate science^{5,6}, economics^{7,8} or online human behaviour⁹. Many real-world systems are thus described as multivariate time-series of (possibly) interlinked processes tracking the temporal evolution (deterministic or random) of groups of observables of interest. The relationships between the measured variables are often complex, in many cases displaying inter-dependencies among each other. For example, the spreading of Covid-19 in Indonesia was dependent on weather conditions¹⁰; the Sustainable Development Goals¹¹ have extensive interlinkages; there are strong interconnections between foreign exchange and cryptocurrencies¹²; and the brain displays multiple spatial and temporal scales of functional connectivity¹³. Driven by technological advances (e.g., imaging techniques in the brain sciences, or the increased connectivity of personal devices via the Internet of Things¹⁴), there is a rapid expansion in the collection and storage of multivariate time-series data sets, which underlines the need for mathematical tools to analyze the interdependencies within complex high-dimensional time-series data.

Characterising the relationships between variables in a multivariate data set often underpins the subsequent application of statistical and machine learning methods. In particular, before further analyses can be performed, it is often crucial to determine whether the variables of interest are jointly independent¹⁵. Joint independence of a set of d variables means that no subset of the d variables are dependent. We need not look further than ANOVA and t-tests to find classic statistical methods that assume joint independence of input variables, and the violation of this assumption can lead to incorrect conclusions. Causal discovery methods, such as structural equation modelling, also require joint independence of noise variables¹⁶. Furthermore, joint independence has applications in uncovering higher-order networks, an emergent area highlighted in recent studies^{17–20}.

Kernel-based methods offer a promising framework for testing statistical independence. Notably, the d -variable Hilbert-Schmidt independence criterion (dHSIC)¹⁶ can be used as a statistic to test the

joint independence of d random variables. Developed as an extension of the pairwise HSIC²¹, dHSIC can be simply defined as the “squared distance” between the joint distribution and the product of univariate marginals when they are embedded in a reproducing kernel Hilbert space (RKHS). Crucially, kernel methods do not make assumptions about the underlying distributions or type of dependencies (i.e., they are non-parametric). Yet, in its original form, dHSIC assumes the data to be *iid* (i.e., drawn from identical independent distributions). This is an unreasonable assumption in the case of time-series data, and it has precluded its application to temporal data.

To the best of our knowledge, dHSIC has not yet been extended to random processes. The pairwise HSIC has been extended to deal with *stationary* random processes under two different test resampling strategies: shifting within time-series²², and the Wild Bootstrap method²³. However, the assumption of stationarity, by which the statistical properties (e.g., mean, variance, autocorrelation) of the time-series are assumed not to change over time, is severely restrictive in many real-world scenarios, as non-stationary processes are prevalent in many areas, e.g., stock prices under regime changes or weather data affected by seasonality or long-term trends. Hence there is a need for independence tests that apply to both stationary and non-stationary processes. Recently, pairwise HSIC has been extended to non-stationary random processes by using random permutations over independent realisations of each time-series, when available²⁴.

In this paper, we show how dHSIC can be applied to reject joint independence in the case of both stationary and nonstationary multivariate random processes. We introduce statistical tests that rely on two different resampling methods to generate appropriate null distributions: one for single-realisation time-series, which is only applicable to stationary random processes, and another for multiple realisation time-series, which is applicable to both stationary and non-stationary random processes. We show numerically that the proposed dHSIC tests on dHSIC identify robustly and efficiently the lack of joint independence in synthetic examples with known ground truths. We further show how recursive testing from pairwise to d -order joint independence can reveal higher-order dependencies in real-world socio-economic time-series that cannot be explained by lower order factorisations.

2 dHSIC for Random Processes

Consider the joint distribution $\mathbb{P}_{\mathbf{X}^1, \dots, \mathbf{X}^d}$ of the random vector $(\mathbf{X}^1, \dots, \mathbf{X}^d)$, where $(\mathbf{X}^1, \dots, \mathbf{X}^d)$ are jointly independent if and only if $\mathbb{P}_{\mathbf{X}^1, \dots, \mathbf{X}^d} = \mathbb{P}_{\mathbf{X}^1} \otimes \dots \otimes \mathbb{P}_{\mathbf{X}^d}$. This implies that any subset of the elements in the random vector are also independent, e.g. $\mathbb{P}_{\mathbf{X}^1, \mathbf{X}^2, \mathbf{X}^3} = \mathbb{P}_{\mathbf{X}^1} \otimes \mathbb{P}_{\mathbf{X}^2} \otimes \mathbb{P}_{\mathbf{X}^3}$ implies $\mathbb{P}_{\mathbf{X}^1, \mathbf{X}^2} = \mathbb{P}_{\mathbf{X}^1} \otimes \mathbb{P}_{\mathbf{X}^2}$ as one can easily integrate with respect to \mathbf{X}^3 on both sides. The contrapositive of this implies that any dependence between a subset of the elements will result in dependence in the whole random vector.

2.1 Joint independence criterion

Let $\{\mathbf{X}_t^j\}$ denote a stochastic process with the probability law $\mathbb{P}_{\mathbf{X}^j}$ for $j \in \{1, \dots, d\}$. We assume that we observe n independent realisations of $\{\mathbf{X}_t^j\}$ in the form of time-series measured at $T_{\mathbf{X}^j}$, i.e. the data samples $\mathbf{X}^j = \{\mathbf{x}_i^j\}_{i=1}^n \stackrel{\text{iid}}{\sim} \mathbb{P}_{\mathbf{X}^j}$ are a set of time-series $\mathbf{x}_i^j = \{x_{i,1}^j, \dots, x_{i,T_{\mathbf{X}^j}}^j\}$. Note that for arbitrary j , the measurements $\{x_{i,t}^j\}$ are not independent across time but rather for fixed time t , the realisations of each variable are independent, i.e. $x_{i_1,t}^j \perp\!\!\!\perp x_{i_2,t}^j \forall t$ and $\forall i_1 \neq i_2$. Consequently, we can represent these distributions by their mean embeddings $\mu_{\mathbf{X}^j}$ in reproducing kernel Hilbert spaces (RKHS) and use it to conduct independence tests. Given a characteristic kernel k , i.e., the mean embedding μ captures all information of a distribution \mathbb{P} , the dependence between measurements in time is captured by the ordering of the variables, and the fact that any characteristic kernel k is injective, thus guaranteeing a unique mapping of any probability distribution into a RKHS²⁵.

All tests requires the time-series to have the same number of realisations n , however a different number of time measurements $T_{\mathbf{X}^j}$ are accepted except when $n = 1$ (single realisation case) with the assumption of stationarity.

2.2 dHSIC for single realisation

Let $\mathbb{P}_{\mathbf{X}^1, \dots, \mathbf{X}^d}$ denote the joint distribution of $\{\mathbf{X}_t^j\}$ and for each \mathbf{X}_t^j let \mathcal{H}_{k^j} be the separable RKHS with characteristic kernel $k^j : \mathbb{R} \times \mathbb{R} \rightarrow \mathbb{R}$, such as the Gaussian kernel. The dHSIC that measures the similarity between the joint distribution and the product of the marginals is defined as:

$$\text{dHSIC}(\mathcal{H}_{k^1} \otimes \dots \otimes \mathcal{H}_{k^d}, \mathbb{P}_{\mathbf{X}^1, \dots, \mathbf{X}^d}) := \|\mu_{\mathbb{P}_{\mathbf{X}^1, \dots, \mathbf{X}^d}} - \mu_{\mathbb{P}_{\mathbf{X}^1} \otimes \dots \otimes \mathbb{P}_{\mathbf{X}^d}}\|_{\mathcal{H}_{k^1} \otimes \dots \otimes \mathcal{H}_{k^d}} \quad (1)$$

where \otimes is the tensor product.

Given only one realisation of \mathbf{X}^j for all $j \in \{1, \dots, d\}$, recall that we assume an equal number of time measurements $T_{\mathbf{X}^1} = \dots = T_{\mathbf{X}^d} = T$ for all d processes, and let $\mathbf{K}^j \in \mathbf{R}^{T \times T}$ be the kernel matrices with entries $k_{ab}^j = k^j(x_{1,a}^j, x_{1,b}^j)$ for $a, b \in \{1, \dots, T\}$. Given one realisation of the $(\mathbf{X}^1, \dots, \mathbf{X}^d)$, without loss of generality \mathbf{x}_1^j , dHSIC is estimated as¹⁶:

$$\widehat{\text{dHSIC}}(\mathbf{X}^1, \dots, \mathbf{X}^d) := \frac{1}{n^2} \sum_{M_2(n)} \prod_{j=1}^d k^j(x_{1,t_1}^j, x_{1,t_2}^j) + \frac{1}{n^{2d}} \sum_{M_{2d}(n)} \prod_{j=1}^d k^j(x_{1,t_{2j-1}}^j, x_{1,t_{2j}}^j) \quad (2)$$

$$- \frac{2}{n^{d+1}} \sum_{M_{d+1}(n)} \prod_{j=1}^d k^j(x_{1,t_1}^j, x_{1,t_{j+1}}^j) \quad (3)$$

where $M_q(n) = \{1, \dots, n\}^q$ and k^j is the kernel for \mathbf{X}^j .

To test the statistical significance of $\widehat{\text{dHSIC}}(\mathbf{X}^1, \dots, \mathbf{X}^d)$, we define the null hypothesis $H_0 : \mathbb{P}_{\mathbf{X}^1, \dots, \mathbf{X}^d} = \mathbb{P}_{\mathbf{X}^1} \otimes \dots \otimes \mathbb{P}_{\mathbf{X}^d}$. Given the significance level α , the threshold c_α for the test statistic can be approximated with a shifting resampling method.

Due to the lack of information provided in the stochastic processes of a single realisation, we need the processes to be strictly stationary²². We fix one time-series and shift all the other $d-1$ time-series as illustrated in Figure 1A. The shifted process $\mathbf{X}_{1,t}^{j,c^j} = \mathbf{X}_{1,t+c^j \bmod T}^j$ is first defined for an integer c^j , $0 \leq c^j \leq T$ and $0 \leq t \leq T$. The null distribution is correctly approximated because the shifted processes breaks the dependence across processes, yet it retains all the local temporal dependence and most of the global dependence within each time-series. We generate the shifted samples $\{\mathbf{X}_s^2, \dots, \mathbf{X}_s^d\}$, $s \in [1, S]$ where S is the number of shiftings, whilst the \mathbf{X}^1 are kept unchanged. $\widehat{\text{dHSIC}}$ is then computed for each shifting and the empirical threshold \hat{c}_α is taken as the statistic as the statistic at position $(1 - \alpha) \times S$. The null distribution is rejected if $\widehat{\text{dHSIC}}(\mathbf{X}^1, \dots, \mathbf{X}^d) > \hat{c}_\alpha$.

We note that there exists an alternative to shifting called Wild Bootstrap^{23,26} which was developed to simulate the null distribution. Unfortunately, Wild Bootstrap has been reported to produce large false positive rates in the absence of dependence²⁷ and therefore we have not used it in this manuscript.

Figure 1: Schematic of the two considered resampling strategies for constructing a null distribution. In both strategies the different colours correspond to variables for which we are interested in testing independence. (A) The shifting method is for strictly stationary time-series data and is useful when only one realisation of each variable is available. For each null sample a random index is chosen for each variable and the two sections (denoted by darker and lighter shades of colour) either side of the index are switched. (B) The permutation method can be applied when multiple realisations of either stationary or non-stationary time-series data is available. Note that this approach is similar to the permutation strategy for *iid* data. For a given null sample, time-series are randomly permuted between realisations indicated by the dotted lines. Null distributions are generated by repeating the chosen method multiple times. In both resampling strategies the first time-series can remain fixed (indicated by dashed line).

2.3 dHSIC for multiple realisations

In the setting where we have multiple independent realisations, we can view each realisation as a sample taken from a multivariate probability distribution. By doing so, the limiting constraints of same point-in-time measurements and stationarity can be loosened.

Let $\mathbb{P}_{\mathbf{X}^1, \dots, \mathbf{X}^d}$ denote the joint distribution of $\{\mathbf{X}_t^j\}$ and for each \mathbf{X}_t^j let \mathcal{H}_{k^j} be the separable RKHS with characteristic kernel $k^j : \mathbb{R}^{T \times j} \times \mathbb{R}^{T \times j} \rightarrow \mathbb{R}$, such as the Gaussian kernel. The dHSIC that measures the similarity between the joint distribution and the product of the marginals is defined similarly as in Eqn. 1.

Given multiple realisations of \mathbf{X}^j for all $j \in \{1, \dots, d\}$, let $\mathbf{K}^j \in \mathbb{R}^{n \times n}$ be the kernel matrices with entries $k_{ab}^j = k^j(\mathbf{x}_a^j, \mathbf{x}_b^j)$ for $a, b \in \{1, \dots, n\}$. Given n iid realisations of the $(\mathbf{X}^1, \dots, \mathbf{X}^d)$, dHSIC is estimated as¹⁶:

$$\widehat{\text{dHSIC}}(\mathbf{X}_1, \dots, \mathbf{X}_d) := \frac{1}{n^2} \sum_{M_2(n)} \prod_{j=1}^d k^j(\mathbf{x}_{i_1}^j, \mathbf{x}_{i_2}^j) + \frac{1}{n^{2d}} \sum_{M_{2d}(n)} \prod_{j=1}^d k^j(\mathbf{x}_{i_{2j-1}}^j, \mathbf{x}_{i_{2j}}^j) \quad (4)$$

$$- \frac{2}{n^{d+1}} \sum_{M_{d+1}(n)} \prod_{j=1}^d k^j(\mathbf{x}_{i_1}^j, \mathbf{x}_{i_{j+1}}^j) \quad (5)$$

We repeat the test hypothesis as outlined in Section 2.2. Here a different resampling method, permutation test is used due to the presence of multiple realisations as illustrated in Figure 1B. Again fix one random process, but for the rest of the processes, instead of shifting the time-series, we randomly permute $\{\mathbf{x}_i^j\}_{i=2}^n, \dots, \{\mathbf{x}_i^j\}_{i=d}^n$, resulting $\{\mathbf{X}_p^2, \dots, \mathbf{X}_p^d\}$, $p \in [1, P]$ where P is the number of permutations. $\widehat{\text{dHSIC}}$ is then computed for each shifting and the empirical threshold \hat{c}_α is taken as the statistic at position $(1 - \alpha) \times P$. The null distribution is rejected if $\widehat{\text{dHSIC}}(\mathbf{X}^1, \dots, \mathbf{X}^d) > \hat{c}_\alpha$.

2.4 Identifying higher-order dependence

Testing joint independence of d -variables offers us an opportunity to define a recursive framework for identifying higher-order dependence. To identify higher-order dependence we implement an extensive search of the dependence between d variables from order 2 to order d . As soon as the test rejects the joint independence of order $m < d$, we stop as the tests from order $m + 1$ to d will also reject the joint independence hypotheses. With the same recursive formulation, we can identify groups of d -variables for which joint independence is rejected but any subset of $(m < d)$ -variables are independent, thus identifying *higher-order dependencies* that cannot be factorised or explained by lower order dependencies. We emphasise here that the rejection of an independence test isn't sufficient evidence to define dependence, and therefore our definition of higher-order dependence is not exact, However, we believe it is still of interest to the reader and apply it within the results section.

3 Results for single realisation time-series

In this section, we empirically evaluate dHSIC for single-realisation datasets using the shifting method for generating the null distribution. We first run experiments on toy examples some of which are sourced from²⁸, calculating the percentage of times that the null hypothesis is rejected for differing lengths of time-series. We then further validate our method on synthetic frequency mixing data with a known ground truth and finally we explore the dependency between variables in real PM2.5 air quality data.

3.1 Validation on toy examples

To validate our approach on toy examples, we define the null hypothesis for 3-way independence as $H_0 : P_{XYZ} = P_X P_Y P_Z$. We compute each test with $P = 1000$ null resampling iterations to approximate the null distribution under H_0 and use a 5% significance level unless otherwise indicated. For each example experiment we generated 200 datasets, where each dataset consists of T consecutive time measurements for each variable with varying dependence coefficient, Figure 2. The test power is calculated for varying the length of time-series $T = [100, 300, 600, 900, 1200]$ and the dependence coefficient d . We further calculate the corresponding confidence intervals (over the 200 repeated datasets) are computed via $\hat{\mu} \pm 1.96 \sqrt{\hat{\mu}(1 - \hat{\mu})/200}$ and illustrated as the shaded area in the figures.

3.1.1 Effect of time-series length on test power

Our first stationary toy example is taken from²⁸ and includes a 3-way dependence without any underlying pairwise relationships (Figure 2A). It is defined as,

$$X_t = \frac{1}{2}X_{t-1} + \epsilon_t, \quad Y_t = \frac{1}{2}Y_{t-1} + \eta_t, \quad Z_t = \frac{1}{2}Z_{t-1} + d|\theta_t|\text{sign}(X_t Y_t) + \zeta_t, \quad (6)$$

where $\theta_t, \eta_t, \zeta_t$ and ϵ_t are generated from $N(0, 1)$, and d is the dependence coefficient. As expected, and ignoring some minor fluctuations for $T = 100$, the power of the test increases with the dependence coefficient. For sufficiently large T , full power can be achieved with relatively low dependence.

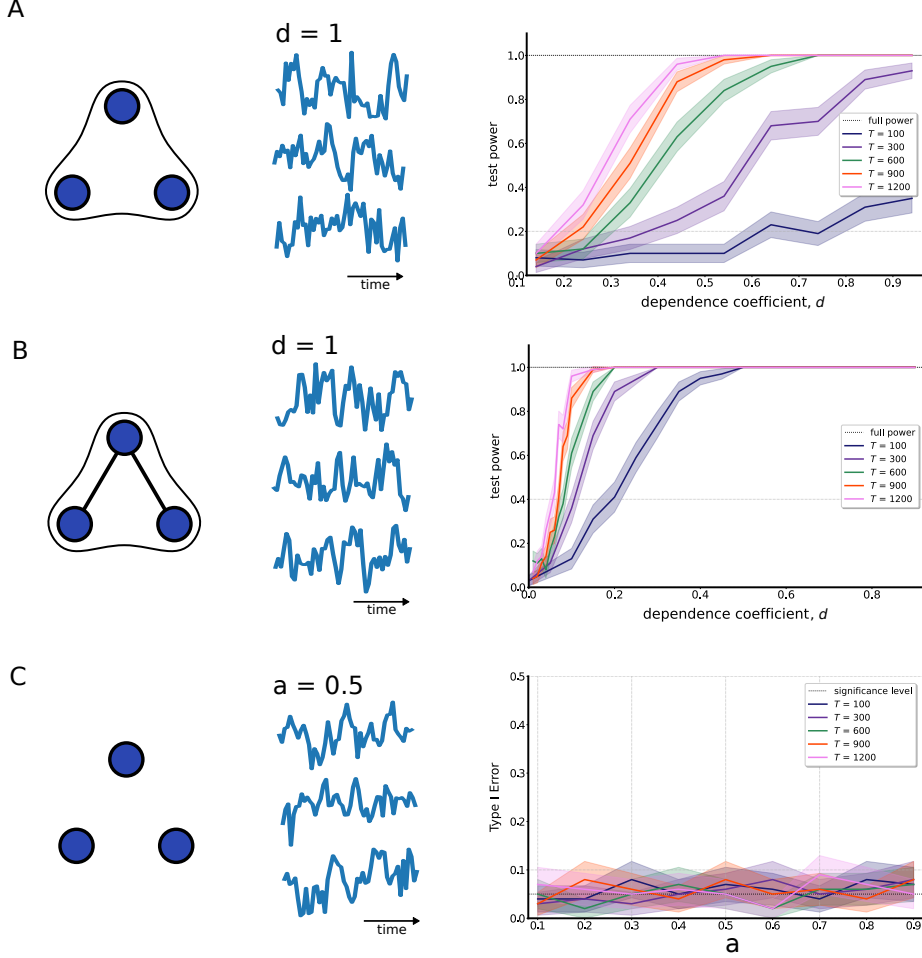


Figure 2: **Three-variable toy examples of stationary data with single realisations.** Left, a visualisation of the true dependences where edges represent pairwise dependence and 3-edges represent 3-way dependence. Middle, an example of the time-series for which dHSIC was computed. Right, the test power (type-1 error for C) for increasing dependence coefficient d (a for C) for different length of time-series T . (A) Genuine 3-way dependence with no underlying pairwise dependences. (B) Pairwise and 3-way dependence. (C) Total independence between variables.²⁸ We note that a is a parameter in the function and should not be confused with the critical value α .

The second stationary toy example is taken from²⁸ and includes simultaneously two pairwise dependences and a 3-way joint dependence,

$$X_t = \frac{1}{2}X_{t-1} + \epsilon_t, \quad Y_t = \frac{1}{2}Y_{t-1} + \eta_t, \quad Z_t = \frac{1}{2}Z_{t-1} + d(X_t + Y_t) + \zeta_t. \quad (7)$$

with equivalent terms to the prior toy example minus θ_t .

Again, we observe that the power increases with the number of time measurements (Figure 2B). Maximum test power is already reached by $d = 0.5$ across all lengths of time-series. In comparison

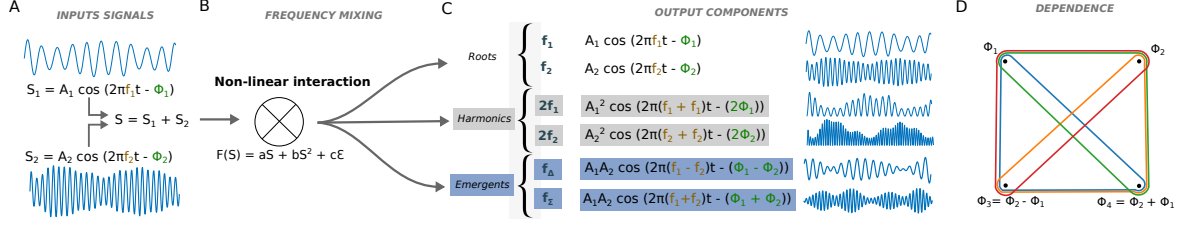


Figure 3: **Frequency mixing example.** (A) Two independent input signals (roots) are generated each with a given dominant frequency (7 Hz and 18 Hz respectively) and amplitude. (B) The signals are mixed using a quadratic function that (C) generates a new signal containing the roots, harmonics (at double the frequency of each root), and emergents at the sum and difference frequency of the roots. Notice that the emergent signals also have a sum and difference in their instantaneous phases. (D) By applying the shifting method with dHSIC to the instantaneous phases of the inputs and the emergent components we reject all pairwise dependences but we do not reject 3-way dependences shown by the 3-edges.

to the first toy example, where the power for $T = 100$ at $d = 0.5$ is only 0.4, this suggests that the joint independence test is more sensitive when the pairwise dependencies are strong.

3.1.2 Effect of time-series length on type I error rate

For a final validation experiment of dHSIC with the shifting method, we used a jointly independent example²⁸,

$$X_t = aX_{t-1} + \epsilon_t, \quad Y_t = aY_{t-1} + \eta_t, \quad Z_t = aZ_{t-1} + \zeta_t. \quad (8)$$

where ϵ_t , η_t and ζ_t are generated from $N(0, 1)$. We show that the Type I error using the shifting resampling method is well-controlled (Figure 2C). By changing the value of a , the type I error stays around 0.05 for all T .

3.2 Synthetic frequency mixing data

As a further illustration linked more closely to real-world applications, we have generated a dataset based on frequency mixing of temporal signals. Frequency mixing is a well known phenomenon in electrical engineering, widely used for heterodyning, i.e., shifting signals from one frequency range to another. Applying a non-linear function such as a quadratic function or a rectifier to two signals at differing frequencies generates new signals at the sum and difference of the input signals (Figure 3A-C). It has previously been shown that the instantaneous phases of the emergent sum and difference signals display a unique 3-way dependence, without any underlying pairwise dependences^{29–31}. Importantly, the instantaneous phase can be considered as a stationary signal given a sufficiently large number of time-series measurements relative to the frequency.

Here, we generated a dataset with two sinusoidal functions with frequencies 7Hz and 18Hz and applied a quadratic function generating a signal which contained the inputs, harmonics and emergents at the sum and difference frequency (see²⁹ for further details). We computed a Wavelet transformation and extracted the instantaneous phases of 7Hz, 11Hz, 18Hz and 25Hz, which can be considered as stationary time-series. Then, we calculated the dHSIC with shifting for $d = [2, 3, 4]$, with $T = 1000$ and $P = 1000$. We found that the null hypotheses were correctly rejected for all tests involving 3 or 4 signal, whilst all variables were pairwise independent. The rejections of the 3-way null hypotheses, without rejections of pairwise hypotheses, recovers our ground truth expected structure (Figure 3D).

3.3 Application to climate data

As an illustration of dHSIC for the single realisation time-series, we applied our approach to the PM2.5 air quality data set. The data set contains hourly measurements of the Particulate Matter 2.5 (PM2.5) recorded by the US Embassy in Beijing between 2010 and 2014. The data set is further supplemented by meteorological data from Beijing Capital International Airport³². We first reduced the number of time measurements by taking the average weekly readings of 4 variables, PM2.5, dew

point (temperature below which dew can form), temperature and air pressure. Non-stationary trends and yearly seasonal effects were removed by differencing of period 1 and period 52, and stationarity was verified by an Adfuller test³³. Unsurprisingly, we find that the null hypothesis of all the independence tests are rejected implying that PM2.5, dew point, temperature and air pressure are all dependent on each other.

4 Results for multiple realisation time-series

In this section, we empirically evaluate dHSIC for multiple-realisation datasets using the permutation resampling method for generating the null distribution. We first run experiments on toy examples with varying non-stationary behaviour, calculating the percentage of rejections of the null hypothesis for differing length of time-series. We then further validate our method on synthetic XOR data with known ground truth and finally we explore the dependency between variables in real Sustainable Development Goal (SDG) data.

4.1 Validation on non-stationary toy examples

To validate our approach on non-stationary toy examples, we define the null hypothesis for 3-way independence as $H_0 : P_{XYZ} = P_X P_Y P_Z$. For each example experiment we generated 200 datasets, where each dataset consists of T consecutive time measurements and N realisations for each variable with varying dependence coefficient, Figure 4. The test power is calculated for varying the length of time-series $T = [1, 3, 5, 10, 20]$ (with $N = 40$ fixed), for varying numbers of realisations $N = [20, 30, 40, 50, 100]$ (with $T = 20$ fixed) and the dependence coefficient d . We further calculate the corresponding confidence intervals (over the 200 repeated datasets) are computed via $\hat{\mu} \pm 1.96\sqrt{\hat{\mu}(1-\hat{\mu})/200}$ and illustrated as the shaded area in the figures.

We perform 4 experiments, wherein the first three display a 3-way joint dependence and two pairwise dependences simultaneously (Figure 4A-C). The first displays a linear trend (Figure 4A),

$$X_t = X_{t-1} + t + \epsilon_t \quad Y_t = Y_{t-1} + t + \eta_t \quad Z_t = Z_{t-1} + t + d(X_t + Y_t) + \zeta_t \quad (9)$$

whilst the second displays a nonlinear trend (Figure 4B), and the third a complex non-linear trend (Figure 4C) (for the functional relationships see Methods and for additional examples see SI). Similar to the stationary toy examples in the previous section, we find that increasing time measurements rapidly improves test power at lower dependence coefficients and, as expected, increasing the number of realisations N also improves the test power. Its important to notice that for $T = 1$, we are unable to reject the null hypotheses regardless of dependence strength as the temporal dependence is no longer observable.

For the final non-stationary toy experiment, we have chosen a pure 3-way dependence (Figure 4D),

$$X_t = aX_{t-1} + t \sin(t) + \epsilon_t \quad Y_t = aY_{t-1} + t \cos(t) + \eta_t \quad Z_t = aZ_{t-1} + dt(X_t + Y_t) + \zeta_t \quad (10)$$

where we set $a = 0.8$, the point at which the data becomes non-stationary according to Ad Fuller test. Again, we observe an increasing test power for more time measurements, but we find that the test power plateaus below full power for $N < 100$. Similarly to the pure high-order stationary example (Figure 2A), the test power is significantly weaker relative to the examples with pairwise dependences present, suggesting that it is more difficult to reject the null hypothesis when only a high-order dependence is present.

4.2 Synthetic XOR dependence

As another form of validation for dHSIC on non-stationary data, we have generated boolean time-series data with dependence driven by an Exclusive OR (XOR) gate dependence. When a single input is 1 then the XOR gate will return 1, however, if both or neither of its inputs are 1, then the XOR gate will return 0. Here, X_0, Y_0, W_0, Z_0 are randomly generated boolean variables with added noise

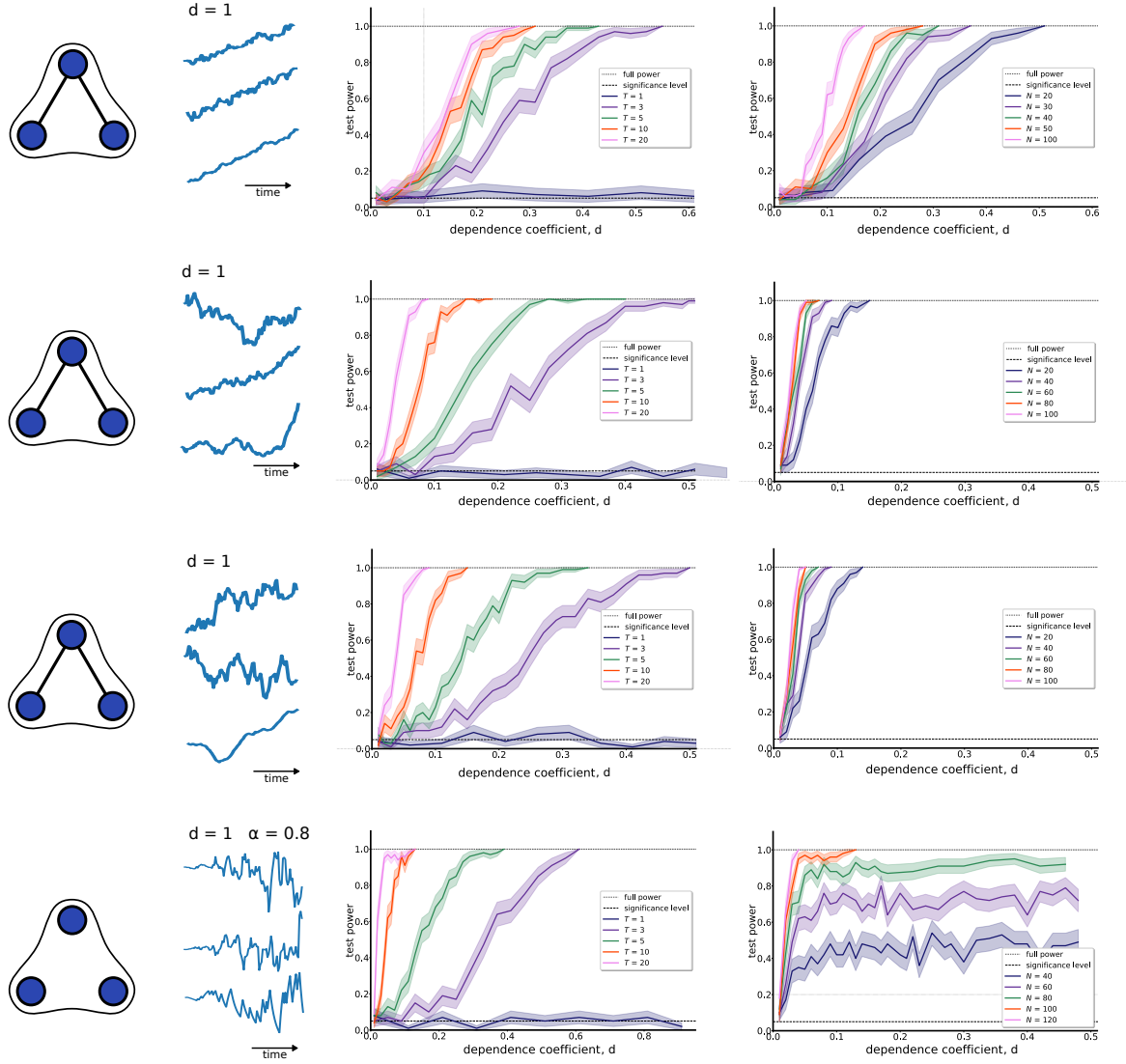


Figure 4: **Three-variable toy examples of non-stationary data with multiple realisations.** Left, a visualisation of the true dependences where edges represent pairwise dependence and 3-edges represent 3-way dependence. Middle left, an example of the non-stationary time-series for which dHSIC was computed. Middle right, the test power for increasing dependence coefficient d for increasing length of time-series T (fixed $N =$) and, right, for increasing number of realisations (fixed $T =$). (A)-(C) Pairwise and 3-way dependence with (A) a linear trend, (B) a complex non-linear trend, and (C) an arbitrary complex trend with perturbed dependence term. (D) Genuine 3-way dependence with no underlying pairwise dependencies ($\alpha = 0.8$ determines when the data becomes non-stationary).

$n_{X_t}, n_{Y_t}, n_{W_t}, n_{Z_t}$ generated from a uniform distribution between 0 and 1,

$$\begin{aligned}
 X_t &= \begin{cases} X_{t-1}, & \text{if } n_{X_t} \geq 0.5 \\ 1 - X_{t-1}, & \text{otherwise} \end{cases} \\
 Y_t &= \begin{cases} Y_{t-1}, & \text{if } n_{Y_t} \geq 0.5 \\ 1 - Y_{t-1}, & \text{otherwise} \end{cases} \\
 W_t &= \begin{cases} W_{t-1}, & \text{if } n_{W_t} \geq 0.5 \\ 1 - W_{t-1}, & \text{otherwise} \end{cases} \\
 Z_t &= \begin{cases} X_t \oplus Y_t \oplus W_t, & \text{if } n_{Z_t} \geq 0.5 \\ 1 - X_t \oplus Y_t \oplus W_t, & \text{otherwise} \end{cases}
 \end{aligned} \tag{11}$$

where \oplus is the XOR gate. When the noise falls under 0.05 then the boolean values are flipped. As expected, our tests do not reject the independence for $d = [2, 3]$ order dependences, but do reject independence of the 4-variable case.

4.3 Application to Socioeconomic data

As a final illustration of our method, we apply it to the United Nations’ socioeconomic Sustainable Development Goals (SDGs) data set³⁴, consisting of 17 SDGs measured from 2000 to 2019. In particular, we investigate the independence of the 17 SDG’s, assuming that countries are independent realisations. For comparison, we divide the countries based on income level: 74 countries with low and lower middle income and 105 countries with high and upper middle income. We also split countries based on geography: 49 countries in the Global North and 137 countries in the Global South.

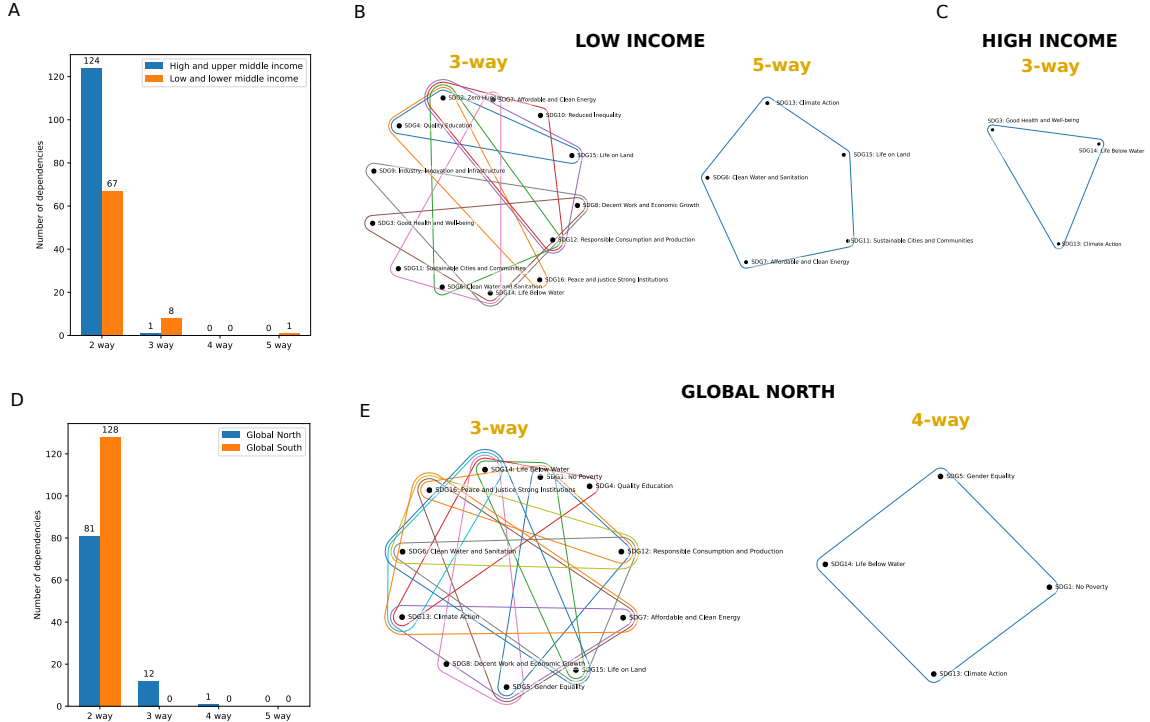


Figure 5: Uncovering the dependences of sustainable development goals. (A-C) A comparison of SDG dependences for low and high income countries. (A) The dependencies for varying orders reveals a shift towards higher-order dependences in low-income countries. The $d > 2$ dependences are mapped onto d -order hypergraphs for (B) low-income and (C) high-income countries. (D-E) A comparison of SDG dependences for countries geographically split by global north and global south. (A) The dependencies for varying orders reveals a shift towards higher-order dependences in global north countries. The $d > 2$ dependences are mapped onto d -order hypergraphs.

We find that lower income countries display more higher-order dependences (independence tests that cannot be rejected) than higher income countries. Notably, we find eight 3-way dependences and even a 5-way dependence between SDG’s for lower income countries, and only a single 3-way dependence for higher income countries. These results suggest that the relationships between SDGs are far more complicated for lower income countries, an aspect that policy makers should carefully consider. Dividing the countries by global geography also returned interesting results; only the global north region displayed higher-order dependences that weren’t rejected by dHSIC tests. Interestingly, two SDGs, climate action and life below water, have consistently appeared in higher-order dependences with other variables (in lower income, higher income, and in the global north groups).

4.4 Robustness of test power to number of resampling iterations

The test statistic, dHSIC can be computed in $\mathcal{O}(dn^2)$ where d is the number of variables and n^2 is the size of the kernel matrices¹⁶. To test the limitations of dHSIC and time-series data, we varied the number of null samples for each resampling strategy. It is immediately clear that in both cases increasing the number of permutations beyond 100 – 150 does not guarantee greater test power, a result that has been previously discussed for *iid* data³⁵.

5 Discussion

In this paper, we present extensions of the dHSIC method to address the challenge of identifying joint independence in both stationary and non-stationary time-series data. For single realisations of stationary time-series, we employ a shifting method as a resampling technique. In the case of multiple realisations of either stationary or non-stationary time-series, we consider each realization as an independent sample from a multivariate probability distribution, enabling us to utilise random permutation as a resampling strategy. To validate our approach, we conducted experiments on diverse toy and synthetic examples, successfully recovering ground truth relationships. Notably, we have implemented a variety of non-stationary behaviours and show that our multi-realisation resampling strategy is able to identify dependencies irrespective of non-stationary behaviour. Furthermore, as illustrated by our applications to Climate data and Sustainable Development Goal data, the testing framework proposed here is applicable to many scientific areas in which either stationary or non-stationary random processes are the norm.

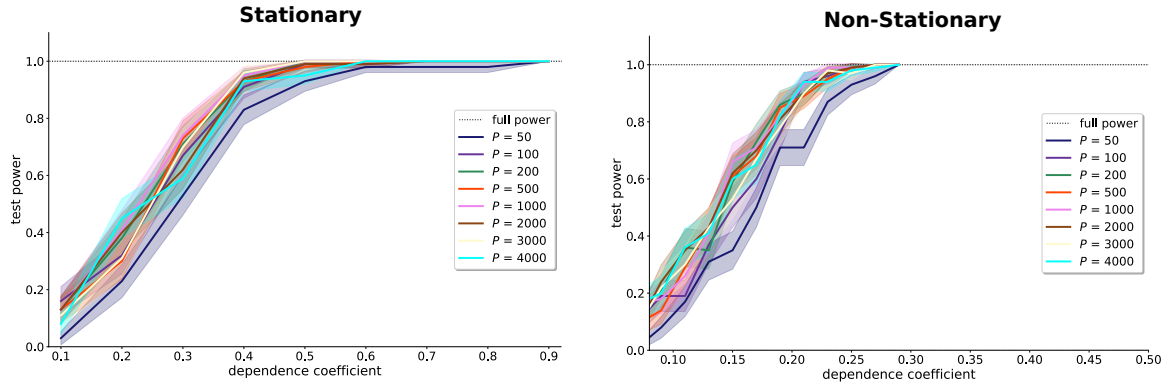


Figure 6: **Testing the robustness of the null distributions.** The test power is computed for varying dependence coefficient for stationary (shifting resampling method) and non-stationary (permutation between multiple realisations) examples. We varied the number of null samples P , showing that relatively few null samples are necessary to attain high test power, i.e., $P > 100$ seems satisfactory for these examples.

While we have conducted thorough numerical validations using diverse datasets of varying complexity, certain aspects related to the efficiency and statistical power of our tests remain unresolved. Our findings highlight the significance of a crucial hyperparameter: the number of resampling iterations required to generate an adequate null distribution. Achieving a delicate balance between test power and computational efficiency becomes paramount, particularly when dealing with large multivariate time-series datasets. The computational costs of our methodology grow linearly in relation to the number of resampling iterations. However, notable differences arise when comparing, for instance, 150 iterations to 10,000 iterations. Our experiments, as depicted in Figure 6, demonstrate that the test power increases with larger numbers of permutations, up to a certain threshold of 150 resampling iterations. Beyond this threshold, further resampling does not necessarily enhance the test power. Determining the optimal number of permutations analytically warrants further investigation and is left as a potential avenue for future research.

It is worth noting that in the case of stationary data with multiple independent realizations, either of the two schemes can theoretically be employed to characterise joint independence. Using the shifting scheme, we can generate a mean time-series by averaging the realisations. Intuitively, when

the number of realisations (N) is much larger than the length of the time-series (T), the permutation strategy is preferred. This strategy naturally aligns with iid permutation approaches and effectively leverages more information from the raw data. Conversely, when N is significantly smaller than T , the strategy of shifting through time measurements becomes more reasonable. It allows for meaningful exploration of the temporal dynamics. In cases where N and T are of comparable magnitude, the choice between resampling strategies is not evident, and further investigation is necessary. We leave such an exploration as a further avenue of future research.

The interest in higher-order networks, such as hypergraphs or simplicial complexes, has been steadily growing²⁰ with applications across various scientific fields^{19,36–39}. Constructing higher-order networks becomes straightforward when relational data naturally establishes links between d entities^{40,41}. However, there is a scarcity of research and a lack of consensus on constructing higher-order networks from observed *iid* or time-series data^{17,42}. In this regard, we believe that the methods proposed in this paper offer a promising avenue for the construction of higher-order networks. By iteratively testing the transition from pairwise independence to d -order joint independence, our approach allows us to uncover dependencies that cannot be explained by lower-order relationships. This framework presents a potential direction for the development of higher-order networks, bridging the gap between observed data and the construction of meaningful network structures.

Acknowledgements

MB acknowledges support by the EPSRC under grant EP/N014529/1 funding the EPSRC Centre for Mathematics of Precision Healthcare at Imperial, and by the Nuffield Foundation under the project "The Future of Work and Well-being: The Pissarides Review". RP acknowledges funding through EPSRC award EP/N014529/1 supporting the EPSRC Centre for Mathematics of Precision Healthcare at Imperial and the Deutsche Forschungsgemeinschaft (DFG, German Research Foundation) Project-ID 424778381-TRR 295.

Competing interests

The authors declare no competing interests.

References

1. Fulcher, B. D. & Jones, N. S. hctsa: A Computational Framework for Automated Time-Series Phenotyping Using Massive Feature Extraction. *Cell Systems* **5**, 527–531.e3. ISSN: 2405-4712. <https://www.sciencedirect.com/science/article/pii/S2405471217304386> (2017).
2. Champion, K. *et al.* Data-driven discovery of coordinates and governing equations. *Proceedings of the National Academy of Sciences* **116**, 22445–22451. eprint: <https://www.pnas.org/doi/pdf/10.1073/pnas.1906995116>. <https://www.pnas.org/doi/abs/10.1073/pnas.1906995116> (2019).
3. Liu, Z. & Barahona, M. *Similarity measure for sparse time course data based on Gaussian processes* in *Uncertainty in Artificial Intelligence* (2021), 1332–1341.
4. Saavedra-Garcia, P. *et al.* Systems level profiling of chemotherapy-induced stress resolution in cancer cells reveals druggable trade-offs. *Proceedings of the National Academy of Sciences* **118**, e2018229118 (2021).
5. Duchon, C. & Hale, R. *Time series analysis in meteorology and climatology: an introduction* (John Wiley & Sons, 2012).
6. Katz, R. W. & Skaggs, R. H. On the use of autoregressive-moving average processes to model meteorological time series. *Monthly Weather Review* **109**, 479–484 (1981).
7. Mills, T. C. *Time series techniques for economists* (Cambridge University Press, 1990).
8. Siarni-Namini, S. & Namin, A. S. Forecasting economics and financial time series: ARIMA vs. LSTM. *arXiv preprint arXiv:1803.06386* (2018).

9. Peach, R. L. *et al.* Data-driven unsupervised clustering of online learner behaviour. *npj Science of Learning* **4**, 1–11 (2019).
10. Tosepu, R. *et al.* Correlation between weather and Covid-19 pandemic in Jakarta, Indonesia. *Science of the total environment* **725**, 138436 (2020).
11. Laumann, F. *et al.* Complex interlinkages, key objectives, and nexuses among the Sustainable Development Goals and climate change: a network analysis. *The Lancet Planetary Health* **6**, e422–e430 (2022).
12. Baumöhl, E. Are cryptocurrencies connected to forex? A quantile cross-spectral approach. *Finance Research Letters* **29**, 363–372 (2019).
13. Mokhtari, F. *et al.* Dynamic functional magnetic resonance imaging connectivity tensor decomposition: A new approach to analyze and interpret dynamic brain connectivity. *Brain connectivity* **9**, 95–112 (2019).
14. Miorandi, D. *et al.* Internet of things: Vision, applications and research challenges. *Ad hoc networks* **10**, 1497–1516 (2012).
15. Vogelstein, J. T. *et al.* Discovering and deciphering relationships across disparate data modalities. *Elife* **8**, e41690 (2019).
16. Pfister, N. *et al.* Kernel-based tests for joint independence. *Journal of the Royal Statistical Society: Series B (Statistical Methodology)* **80**, 5–31 (2018).
17. Rosas, F. E. *et al.* Quantifying high-order interdependencies via multivariate extensions of the mutual information. *Physical Review E* **100**, 032305 (2019).
18. Battiston, F. *et al.* The physics of higher-order interactions in complex systems. *Nature Physics* **17**, 1093–1098 (2021).
19. Arnaudon, A. *et al.* Connecting Hodge and Sakaguchi-Kuramoto through a mathematical framework for coupled oscillators on simplicial complexes. *Communications Physics* **5**, 211 (2022).
20. Battiston, F. *et al.* Networks beyond pairwise interactions: structure and dynamics. *Physics Reports* **874**, 1–92 (2020).
21. Gretton, A. *et al.* A kernel statistical test of independence. *Advances in neural information processing systems* **20** (2007).
22. Chwialkowski, K. & Gretton, A. A kernel independence test for random processes in *International Conference on Machine Learning* (2014), 1422–1430.
23. Chwialkowski, K. P., Sejdinovic, D. & Gretton, A. A wild bootstrap for degenerate kernel tests. *Advances in neural information processing systems* **27** (2014).
24. Laumann, F., von Kügelgen, J. & Barahona, M. Non-linear interlinkages and key objectives amongst the Paris Agreement and the Sustainable Development Goals in *ICLR 2020 Workshop on Tackling Climate Change with Machine Learning* (2020). <https://www.climatechange.ai/papers/iclr2020/9>.
25. Muandet, K. *et al.* Kernel mean embedding of distributions: A review and beyond. *Foundations and Trends® in Machine Learning* **10**, 1–141 (2017).
26. Shao, X. The dependent wild bootstrap. *Journal of the American Statistical Association* **105**, 218–235 (2010).
27. Mehta, R. *et al.* Independence Testing for Multivariate Time Series. *arXiv preprint arXiv:1908.06486* (2019).
28. Rubenstein, P. K., Chwialkowski, K. P. & Gretton, A. A kernel test for three-variable interactions with random processes. *arXiv preprint arXiv:1603.00929* (2016).
29. Luff, C. *et al.* The neuron mixer and its impact on human brain dynamics. *bioRxiv* (2023).
30. Haufler, D. & Paré, D. Detection of multiway gamma coordination reveals how frequency mixing shapes neural dynamics. *Neuron* **101**, 603–614 (2019).
31. Kleinfeld, D. & Mehta, S. B. Spectral mixing in nervous systems: experimental evidence and biologically plausible circuits. *Progress of Theoretical Physics Supplement* **161**, 86–98 (2006).

32. Liang, X. *et al.* Assessing Beijing’s PM_{2.5} pollution: severity, weather impact, APEC and winter heating. *Proceedings of the Royal Society A: Mathematical, Physical and Engineering Sciences* **471**, 20150257 (2015).
33. Said, S. E. & Dickey, D. A. Testing for unit roots in autoregressive-moving average models of unknown order. *Biometrika* **71**, 599–607 (1984).
34. *World Bank. Sustainable Development Goals. 2020* <https://datacatalog.worldbank.org/dataset/sustainable-development-goals>. Accessed: 2020-01-28.
35. Rindt, D., Sejdinovic, D. & Steinsaltz, D. Consistency of permutation tests of independence using distance covariance, HSIC and dHSIC. *Stat* **10**, e364 (2021).
36. Gao, T. & Li, F. Studying the utility preservation in social network anonymization via persistent homology. *Computers & Security* **77**, 49–64 (2018).
37. Arenzon, J. J. & de Almeida, R. M. Neural networks with high-order connections. *Physical Review E* **48**, 4060 (1993).
38. Sonntag, M. & Teichert, H.-M. Competition hypergraphs. *Discrete Applied Mathematics* **143**, 324–329 (2004).
39. Klamt, S., Haus, U.-U. & Theis, F. Hypergraphs and cellular networks. *PLoS computational biology* **5**, e1000385 (2009).
40. White, J. G. *et al.* The structure of the nervous system of the nematode *Caenorhabditis elegans*. *Philos Trans R Soc Lond B Biol Sci* **314**, 1–340 (1986).
41. Atkin, R. H. *Mathematical structure in human affairs* (Heinemann Educational London, 1974).
42. Schneidman, E. *et al.* Network Information and Connected Correlations. *Phys. Rev. Lett.* **91**, 238701. <https://link.aps.org/doi/10.1103/PhysRevLett.91.238701> (23 Dec. 2003).